British Journal of Cancer (2012) 107, 1534–1546

www.bjcancer.com

Interleukin-1α is the major alarmin of lung epithelial cells released during photodynamic therapy to induce inflammatory mediators in fibroblasts

EC Tracy[1], MJ Bowman[1], BW Henderson[2] and H Baumann*[,1]

[1]Departments of Molecular and Cellular Biology, Roswell Park Cancer Institute, Elm and Carlton Streets, Buffalo, NY 14263, USA; [2]Cell Stress Biology/PDT Center, Roswell Park Cancer Institute, Elm and Carlton Streets, Buffalo, NY 14263, USA

BACKGROUND: Photodynamic therapy (PDT) causes tissue damage that initiates a local inflammatory response. Post-PDT reactions are considered to assist in mobilising the immune system thereby affecting tumour recurrence. The initiating process of the PDT-dependent tissue reaction remains to be determined.

METHODS: Primary cultures of human lung cells were established. The photoreaction mediated by pyropheophorbide-a, at specific subcellular sites and levels resulting in the release of alarmins by epithelial cells (Eps), was defined by immunoblot analyses and expression profiling. The activity of Ep-derived factors to stimulate expression of proinflammatory mediators, including IL-6, and to enhance neutrophil binding by fibroblasts (Fbs) was determined by functional bioassays.

RESULTS: Epithelial cells release IL-1β as the primary Fb-stimulatory activity under basal conditions. Intracellular IL-1α, externalised following photoreaction, accounts for most of the PDT-mediated Fb activation. Expression of IL-1 is subject to increase or loss during oncogenic transformation resulting in altered alarmin functions mobilisable by PDT. Photoreaction by a cell surface-bound photosensitiser (PS) is 10-fold more effective than PSs localised to mitochondria or lysosomes. High-dose intracellular, but not cell surface, photoreaction inactivates IL-1 and reduces Fb stimulation.

CONCLUSION: These *in vitro* data suggest that the subcellular site and intensity of photoreaction influence the magnitude of the stromal cell response to the local damage and, in part, support the relationship of PDT dose and level of post-PDT inflammatory response observed *in vivo*.

British Journal of Cancer (2012) **107,** 1534–1546. doi:10.1038/bjc.2012.429 www.bjcancer.com
Published online 20 September 2012

Keywords: photoreaction; tissue damage; inflammation; pyropheophorbide-a; lung cancer

Photodynamic therapy (PDT) of a tissue lesion represents a confined sterile injury that leads to a local inflammatory response. By selecting a defined concentration and subcellular localisation of a photosensitiser (PS) and by delivering a specific therapeutic light dose, the photoreaction elicits a response in target cells that can range from sub-lethal oxidative reactions to the activation of apoptosis and immediate necrotic cell death (Oleinick *et al*, 2002; Wong *et al*, 2003; Buytaert *et al*, 2007). While killing of target cells, as in the case of cancer, is a major goal, successful treatment outcome also depends on post-PDT processes, such as inflammation, acute phase reaction, recruitment of immune functions, and execution of healing programs (Agostinis *et al*, 2011). Earlier *in vivo* work has shown the causal relationship of PDT-mediated tissue injury with presentation of intracellular epitopes, inflammation, activation of immune cells, and tumour control (Gollnick *et al*, 2003; Kousis *et al*, 2007).

While the inflammatory process to sterile tissue injury has been defined in detail, the involvement of comparable reactions in the response to PDT has been proposed, but remains to be determined (Garg *et al*, 2011). The initiation of the inflammatory process has been ascribed to the action of alarmins that include damage-associated molecular pattern proteins (DAMPs), cytokines and metabolites (Gallucci and Matzinger, 2001; Bianchi, 2007). These molecules preexist in cells and are ready for immediate release upon damage. Based on the concept of passive release, mechanical dissociation of cells and necrotic cell death are considered to be the prevalent processes by which alarmins are presented at sites of tissue injury.

Several abundant intracellular proteins serve as DAMPs and act as first-line alarmins (Foell *et al*, 2007; Lotze *et al*, 2007; Osterloh and Breloer, 2008; Riddell *et al*, 2010). Among these are HSP90 and HSP70, S100 proteins, peroxiredoxin-1 (PRX1), and high-mobility group protein B1 (HMGB1). Damage-associated molecular pattern proteins are recognised by various receptor systems, including Toll-like receptors (TLRs), Nod-like receptors, receptor for advanced glycation end products and other scavenger receptors, and are considered to trigger signalling. Besides DAMPs, intracellular cytokines, such as IL-1α and IL-33, are released upon cellular disintegration (Moussion *et al*, 2008; Cohen *et al*, 2010). These cytokines assume immediate signalling functions via their cognate receptors on neighbouring cells. Additional contributors

*Correspondence: Dr H Baumann;
E-mail: heinz.baumann@roswellpark.org
Received 22 June 2012; revised 29 August 2012; accepted 30 August 2012; published online 20 September 2012

to the local inflammatory reaction are mediators that are either activated from latent pro-forms or are synthesised, such as derivatives of inflammasomes or *de novo*-synthesised proinflammatory cytokines and chemokines (Bryant and Fitzgerald, 2009; Dinarello, 2009). Cells spared by the initial tissue damage are targets of alarmins and include stromal cells, resident tissue macrophages, dendritic cells and chemotactically attracted peripheral blood leucocytes (Gollnick *et al*, 2003; Bianchi, 2007; Bratton and Henson, 2011; Laskin *et al*, 2011). These cells produce the second wave of mediators contributing to the tissue injury response and, following the mediators' systemic distribution, to acute phase reactions at distant organ sites (Baumann and Gauldie, 1994).

This study investigated the relationship of the subcellular site of PDT and PDT dose on the release of alarmins in primary cultures of normal and transformed lung epithelial cells (Eps). The results indicate a highly effective, PDT-dependent communication of alarmin function toward stromal fibroblasts (Fbs) that exceeds the one detectable toward pulmonary macrophages. The data also indicate a magnified cell-damaging effect of PDT and alarmin release when the PS is confined to the cell surface. In contrast, high-dose intracellular photoreaction, despite causing immediate necrotic cell death, results in the inactivation of alarmins and, thus, in a drastically reduced induction of inflammatory mediators in stromal cells.

MATERIALS AND METHODS

Photosensitisers

2-(1-Hexyloxyethyl)-2-devinylpyropheophorbide-a (HPPH) and HPPH-galactose (HPPH-Gal) were generated in the laboratory of Dr R Pandey (Zheng *et al*, 2009) and used as described (Tracy *et al*, 2011).

Cells

Primary cultures of lung cells were generated from surgical specimens obtained from tissue procurement services at RPCI under IRB-approved protocol as described (Loewen *et al*, 2005; Chattopadhyay *et al*, 2007; Tracy *et al*, 2011) and are listed with the laboratory protocol number assigned to each specimen (e.g., L297). Tumour-free lung tissue was the source for 'normal' cell types: alveolar pneumocytes II (N-Ep), fibroblasts (N-Fbs) and macrophages. Airways in resected lung segments were brushed and the collected mucosal tissue was processed to obtain cultures of bronchial Eps (BEC) (Loewen *et al*, 2005). Dissected lung squamous carcinoma or adenocarcinoma served as the source for tumour Eps (T-Eps) and tumour-associated fibroblasts (T-Fbs). As described in detail (Tracy *et al*, 2011), all Ep cultures were selectively grown and maintained in collagen 1-coated culture dishes in serum-free keratinocyte medium supplemented with recombinant EGF, bovine pituitary extract and cholera toxin (KSFM; Invitrogen, Carlsbad, CA, USA). Incubation with PSs, light treatment and post-PDT culturing were performed either in serum-free RPMI or in KSFM that did not contain supplements in order to avoid interference with subsequent bioassays for cytokine activity on Fb or macrophages. Long-term cultures (>10 passages) of T-Ep from surgical adenocarcinoma specimens (T-Ep(L237) and T-Ep(L301)), or from squamous carcinoma xenografts (TEC-1, TEC-2 and TEC-9), were adapted for growth in DMEM containing 10% foetal bovine serum (Tracy *et al*, 2011). A subclonal line of A549 adenocarcinoma cells (ATCC, Manassas, VA, USA) (Chattopadhyay *et al*, 2007) was cultured in DMEM containing 10% foetal bovine serum. Incubation of these established cell lines with PS and light treatment occurred in serum-free DMEM.

Human peripheral blood neutrophils were isolated from the erythrocyte pellet after ficoll-hypaque separation of whole blood (pellet provided by the bone marrow procurement laboratory at RPCI). Following erythrocyte lysis, neutrophils were stained with carboxyfluorescein succinimidyl ester (CFSE; Invitrogen). An IL-1 receptor-negative line of rat hepatoma H-35 cells (Reuber, 1961; Baumann *et al*, 1989) with enhancer-trapped green fluorescent protein (GFP) gene inserted into the fourth intron of the hemopexin gene (unpublished) served as bioassay system for IL-6 activity. Induction of GFP is STAT3-specific and strictly dependent on signalling by IL-6-type cytokine receptors (Immenschuh *et al*, 1995; unpublished).

Photosensitiser uptake and photoreaction

Cells were incubated for 30 min at 37° C with serum-free medium containing defined concentrations of PSs. For exclusive cell surface binding of HPPH-Gal, the cells were incubated for 30 min on ice. Internalisation of PS was achieved by incubating cells in PS-free medium for 4–24 h at 37°. Cell-associated PS was visualised at $\times 100$ magnification on an inverted fluorescence microscope (Zeiss Axiovert 200, Jena, Germany; filter setting λex 410/440 nm and λem 675/750 nm). Fluorescence was recorded with a Q-Imaging camera in a 16-bits per channel format within the linear range of light detection. Fluorescence in full-frame images were quantified by integrating pixel values using ImageQuant TL programme (GE Healthcare Life Science, Pittsburgh, PA, USA), corrected for background (culture without PS) and net values calculated for a uniform 1-s image exposure (termed fluorescence units (FU); $1\,\mathrm{FU} = 1 \times 10^8$ pixel).

Photoreaction was performed by illuminating PS-treated cell cultures in serum-free medium at 37° or 0° C with 665 nm light of an argon-pumped dye laser for 9 min at a dose of 5.6 mW cm^{-2} for a total fluence of 3 J cm^{-2}. Cells were either extracted immediately after light treatment or incubated at 37° for time periods ranging from 2 to 24 h. Conditioned medium (CM) was removed after specified time intervals and replaced by fresh medium. Conditioned medium and adherent cell material were collected for analysis of Fb-stimulatory activity (FSA) and cellular proteins.

Cell analyses

Cells were lysed in radioimmunoprecipitation assay (RIPA) buffer. Aliquots of extracts or CM were subjected to western blotting as described (Liu *et al*, 2004; Chattopadhyay *et al*, 2007; Tracy *et al*, 2011). Membranes were reacted with one of the primary antibodies: STAT3, ERK1/2, cytochrome C, HSP90, or HSP70 (Santa Cruz Biotechnology, Santa Cruz, CA, USA); PY705-STAT3, P-ERK1/2, p38, PT180/PY182-p38, PS536-p65, p65, EGFR, Akt, PS473-Akt, IL-1α (R&D, Minneapolis, MN, USA); HMGB1, CD54/ICAM-1 (Cell Signaling Technology Inc., Danvers, MA, USA); PRX1 (Abnova, Taiwan, ROC); human haptoglobin (Accurate Chemical, Westbury, NY, USA); or actin (Sigma-Aldrich, St Louis, MO, USA). The immune complexes were visualised with peroxidase-coupled secondary antibodies and enhanced chemiluminescence detection (Pierce Chemicals, Rockford, IL, USA). STAT3 crosslinking was expressed by the percentage conversion of monomeric STAT3 into the dimer form I of STAT3 (Liu *et al*, 2004; Henderson *et al*, 2007; Tracy *et al*, 2011). Immunodetectable level of ERK-1/-2 in cell homogenates served as sample loading reference. Viable cells were determined by counting in a hemocytometer using trypan blue exclusion as viability criterion.

Transcript analysis by affymetrix gene chip array

Replicate sets of BEC in 10-cm-diameter dishes were subjected to control and 25 nM HPPH-PDT followed by incubation for 2 and 24 h. Three replicate sets N-Fb cultures were treated for 24 h with growth medium alone or containing 1/10 diluted Ep CM 4 h post 50 nM HPPH-PDT. RNAs were extracted from the cultures and

processed according to the Affymetrix GeneChip Expression Analysis Manual (Affymetrix Inc., Santa Clara, CA, USA) as described (Hawthorn *et al*, 2006). The cRNA samples were hybridised to Human Genome U133 Plus 2.0 Array. Data were normalised (Hawthorn *et al*, 2006) and compared for >two-fold treatment-induced changes in transcripts.

Fibroblast assay for alarmin and IL-1 activity, production of IL-6 and neutrophil binding

Confluent Fb cultures in 48-well plates ($\sim 1 \times 10^5$ cells per well) were treated with DMEM containing 10% fetal bovine serum (150 μl per well) alone or containing either 1/3 to 1/10 diluted Ep CM; 10 ng ml^{-1} of recombinant IL-1β or IL-1α (17 kD; Peprotech, Rocky Hill, NJ, USA); IL-1F9 or IL-33 (R&D); or COS-1 cell-derived IL-1α (17 kD + 31 kD forms; Genetics Institute/Wyeth Research, Boston, MA, USA); 100 ng ml^{-1} oncostatin M (OSM) (Chattopadhyay *et al*, 2007); 100 ng ml^{-1} hyper-IL-6 (Rakemann *et al*, 1999); 1 μg ml^{-1} LPS (Sigma-Aldrich); or 10 μg ml^{-1} heat-killed *Salmonella*. To determine signalling, Fb were extracted after a 15-min treatment and analysed by immunoblotting. To induce ICAM-1 and cytokine genes, Fb were treated for 24 h. Fb CM were collected. Cells were rinsed once with serum-free RPMI and incubated with CSFE-stained neutrophils (2×10^6 in 0.5 ml serum-free RPMI) for 15 min at 37° C. Culture wells were washed four times with serum-free medium. CSFE-fluorescence was scanned in a Typhoon Trio (GE Healthcare Life Sciences) and quantified by ImageQuant TL analysis (GE Healthcare Life Sciences). The integrated pixel value for the entire culture well served as arbitrary unit of CSFE–neutrophil binding in each experimental series. Adherent cells were extracted with RIPA buffer and analysed for ICAM-1 and neutrophil haptoglobin by western blotting. In each experimental series, one culture was treated with 10 ng ml^{-1} IL-1β as a reference for maximal IL-1 response. The amount of IL-6 in CM (or IL-1 in Ep CM) was determined by Luminex immunobead binding/flow cytometry (Luminex, Austin, TX, USA and Bio-Rad, Hercules, CA, USA). Activity of IL-6 in CM was determined by a bioassay on H-35 cells. Monolayers of H-35 cells with enhancer-trapped GFP were treated in 96-well culture plates for 24 h with 100 μl per well of DMEM containing 0.5% fetal bovine serum, 1 μM dexamethasone and serially diluted aliquots of CM. Treatment-induced GFP was quantified by fluorescence imaging in a Typhoon-Trio and ImageQuant analysis. In every assay, serially diluted human IL-6 was included as reference. Maximal GFP induction was defined by the response to 100 ng ml^{-1} IL-6 (half-maximal induction at $\sim$1 ng ml^{-1} IL-6). The amount of IL-6 in test samples (expressed as ng IL-6 released by 1×10^6 cells in 24 h) was calculated based on the dose–response profile to the IL-6 standard. The coupled Fb/H-35 cell assay also allowed quantification of IL-1 in which the dose-dependent induction of IL-6 expression by 10-fold serially diluted Ep CM was compared with that of 10-fold serially diluted IL-1α or IL-1β standards (half-maximal response for both IL-1 forms at $\sim$0.1 ng ml^{-1}). The contribution of IL-1α, IL-1β and IL-6 to the regulatory activities defined by the Fb/H-35 cell assay was determined by inhibition with neutralising antibodies against IL-1α, IL-1β and the common signal-transducing receptor subunit for IL-6-type cytokines, gp130, respectively (R&D).

Size fractionation of cellular protein

Conditioned medium from Ep cultures in 10-cm-diameter dishes were collected 2 h and 24 h after 50 nM HPPH-PDT and concentrated 30-fold. Tumour Ep in a 10-cm dish were scraped in 300 μl PBS and homogenised by ultrasonication. Proteins in centrifuged CM or homogenate were size-separated on a Sephadex G150 column (0.9 × 30 cm; Pharmacia, Uppsala, Sweden) in sterile PBS and collected in 0.5 ml fractions. The elution profile was calibrated by chromatographing reference proteins.

Statistical evaluation

Quantitative results were expressed as mean and s.d., and the significance was evaluated by Student's *t*-test. Box plots of expression data were drawn using the online R programme (http://www.r-project.org/). The results are illustrated with the box indicating median (thick line) and two quartiles (25–75%), whiskers for values within 1.5 interquartile range and dot for outlier.

RESULTS

Fibroblasts as targets of alarmins

Exploratory studies with primary human lung cells and combinations of these in three-dimensional co-cultures indicated a constitutive release of factors by Ep that stimulated Fb to enhance the expression of IL-6. Photodynamic therapy further increased the release of this stimulatory activity, which was termed 'FSA'. Notably, the Ep-derived factors did not appreciably activate pulmonary macrophages. These observations suggested a communication from epithelial to mesenchymal cells that might have a role in the PDT response of lung tissue and that was separate to the minor contribution by macrophages. The current study set the goal to identify this Ep-to-Fb communication.

As the first step in defining this Fb regulation, we determined the specificity by which Fb responded to known irritants and cytokines associated with inflammation and whether the regulatory property was consistent among preparations and passages of N-Fb and T-Fb. This information was necessary because primary Fb cultures were chosen as an assay system for Ep-derived mediators. The activation of intracellular signalling pathways and induction of genes served as markers for the Fb response. Two assays were applied: one determined the activation of signalling pathways by a 15-min treatment (Figure 1A and D, upper 2 panels) and the other measured after 24-h treatment the release of IL-6 activity, enhanced ICAM-1 expression and increased neutrophil binding (Figure 1B–D (lower 2 panels) and E).

While Fb failed to respond to TLR-2, -4 and -5 agonists (LPS and *Salmonella*) by enhanced phosphorylation of p38 stress MAPK and p65/NFκB, the cells activated these pathways when treated with the cytokine combination derived from LPS-activated macrophages. The response to macrophage CM also included signalling through gp130 (STAT3 phosphorylation), in agreement with the predicted combinations of IL-1/TNF/OSM/IL-6 released by activated macrophages (Laskin *et al*, 2011). Epithelial cell CM-stimulated signalling with the hallmarks of IL-1/TNF (phosphorylation of p65/NFkB and p38 MAPK), but without a detectable effect on the gp130 pathway (no measurable STAT3 phosphorylation). Photodynamic therapy enhanced the release of this Ep activity (Figure 1A). Activation of NFκB and p38 by Ep CM or IL-1 was proportionally reflected after 24 h in the induced ICAM-1 expression and enhanced neutrophil binding monitored by CSFE-fluorescence (Figure 1C and D) and detection of neutrophil-derived haptoglobin (Figure 1B).

The regulatory capability of primary Fb cultures was significant and highly reproducible as documented by the maximal induction of IL-6 expression by IL-1β in 12 independently derived N-Fb and T-Fb preparations (Figure 1E). Despite variable basal expression, there was a consistent 10- to100-fold induction in both N-Fb and T-Fb that was independent of passage number. This IL-1 response demarked the testable range for Ep-derived FSA.

PDT-induced presentation of DAMPs and FSA by primary lung Ep

The PDT-dependent release of cellular material was determined on confluent Ep cultures that were incubated for 30 min with HPPH, followed for 24 h with PS-free medium. Within this time period,

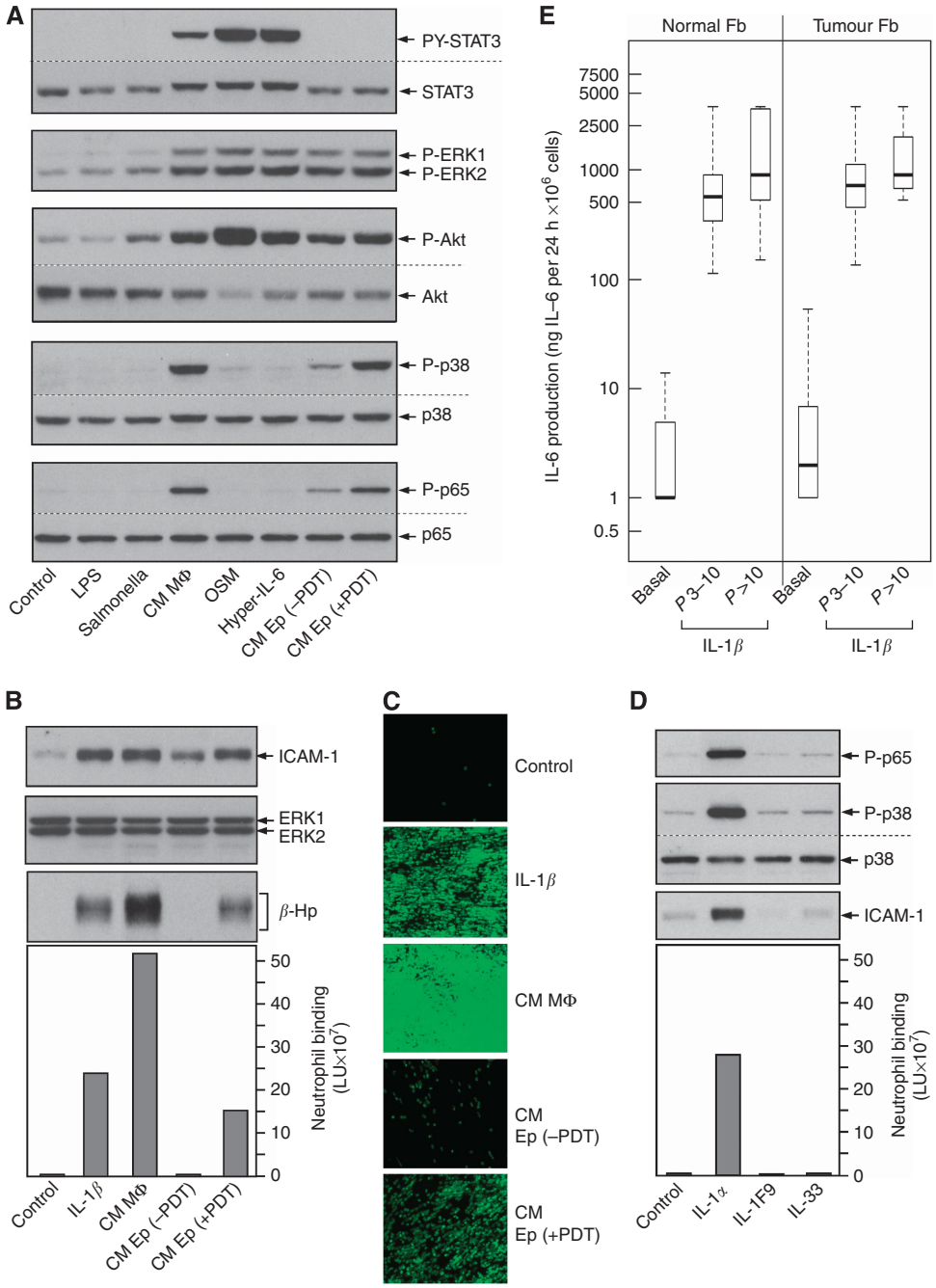

Figure 1 Fibroblasts as target for irritants and alarmins. (**A**) Monolayers of primary cultures of N-Fb, passage 4, were treated for 15 min with the irritants or cytokines listed at the bottom. The changes in the phosphorylation of the signalling proteins indicated on the right were determined by western blotting. (**B, C**) N-Fb were treated for 24 h as indicated and then were exposed for 15 min to CSFE-stained neutrophils. Adherent neutrophils were imaged by CSFE-fluorescence (**B**, bottom panel, and **C**) and the change in the expression of ICAM-1 as well as the neutrophil-associated haptoglobin determined by western blotting (**B**, upper panels). (**D**) separate cultures of N-Fb were treated with the cytokines indicated at the bottom and analysed for the 15-min response to activate NFkB and p38 and for the 24-h response to induce ICAM-1 and binding of CSFE-stained neutrophils. (**E**) Baseline and IL-1β-inducible IL-6 production by early (P3–10) and late (P>10) passage culture of N-Fb and T-Fb were quantified by bioassay and Luminex immunobead-binding assays. Box plots compile data from 8 to 24 independent culture sets.

HPPH reached a steady-state subcellular distribution with predominant localisation to mitochondria (Figure 2A) (Zheng *et al*, 2009). The amount of cellular HPPH was quantified based on fluorescence (Figure 2C). HPPH-mediated photoreaction was evaluated either immediately after light treatment by the oxidative crosslinking of STAT3, loss of EGFR and the activation of p38 MAPK (Figure 2B) or 24 h later by the number of surviving cells (Figure 2C). The results indicated a highly reproducible relationship: under the conditions used to incubate Ep with HPPH, the amount of cell-associated HPPH, yielding ~25 FU, mediated ~1% STAT3 crosslinking and ~50% cell kill, and HPPH, yielding ~50 FU, produced ~2% STAT3 crosslink and 95–100% cell kill. Cell death at HPPH doses <50 FU (or ~25–50 nM) was mostly owing to apoptosis, whereas death by PDT at HPPH doses >50 FU (or >50 nM) was due to necrosis (Liu *et al*, 2004).

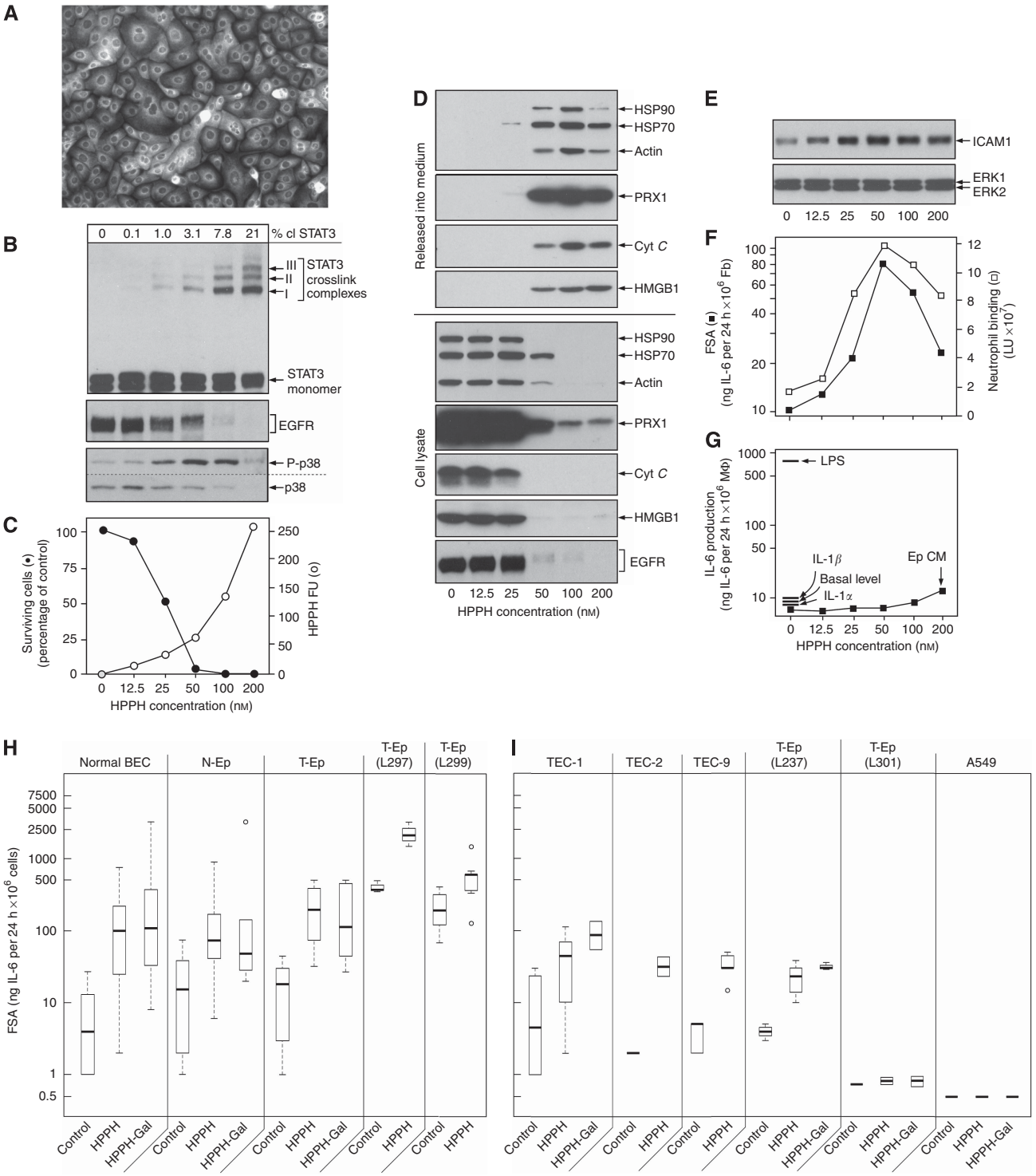

Figure 2 Effect of PDT on lung Eps. (**A–E**) Replicate N-Ep cultures, passage 2, in 6-well culture dishes were incubated for 30 min with the indicated concentrations of HPPH followed by 24 h incubation in HPPH-free medium. Mitochondrially localised HPPH was determined by fluorescent microcopy (**A**, × 100 magnification) and quantified (**C**, open circles). The cultures were exposed to 665 nm light. Cells from one culture set were immediately extracted and analysed for the indicated proteins by western blotting (**B**). The second set of cultures was incubated for an additional 24 h. The relative level of viable cells was determined (**C**, closed circle). Equivalent aliquots of culture supernatant and lysate of adherent cell material were analysed by western blotting for the indicated proteins (**D**). Additional aliquots of conditioned media were 10-fold diluted and used to treat N-Fb in 48-well plate for 24 h (**E, F**). The treatment-dependent change in the cellular expression of ICAM-1 was determined by western blotting (**E**), binding of neutrophils (**F**, open squares, LU×10^7) and release of IL-6 activity determined on H-35 cell assay (**F**, closed squares). The same diluted EC-conditioned media were used to treat primary pulmonary macrophages for 24 h for determining the effect on IL-6 production (**G**). (**H, I)** Primary cultures of BEC ($n = 12$), N-Ep ($n = 12$), T-Ep ($n = 12$) (**H**) and established Ep lines (**I**) were analysed for basal line and PDT-induced (50 nM HPPH or 100 nM HPPH-Gal) release of FSA during the 24-h post-PDT culture period. Box plots represent compilation of data derived from separate cell preparations representing passages 2 to 7 (**H**) and repeat ($n = 3–12$) measurements on individual cultures of established lines for up to passage 90 (**I**).

Cell death was correlated with the loss of cellular proteins from adherent cells and corresponding appearance of these in culture medium (Figure 2D). Release of cellular proteins as a function of PDT dose and cell death is reflected in the immune-detectable amount of cytoplasmic (HSP90, HSP70 and PRX1), mitochondrial (cytochrome *C*) and nuclear (HMGB1) DAMPs. Analyses of cell-free supernatants from Ep cultures on Fb indicated a basal level and PDT-dependent increase of FSA (IL-6 production), expression of ICAM-1 and binding of neutrophils (Figure 2E and F). The recovery of FSA reached a maximum at a PDT dose that correlated with nearly 100% cell death. Higher PDT doses reduced FSA despite more abundant DAMP release (Figure 2F).

To assess whether Ep CM contained irritant-like activity attributable to DAMPs, including ligands for TLR-2, -4 and -5, we tested the same culture supernatant on primary pulmonary macrophages (Figure 2G). Although these cells are highly effective in recognising irritants, such as LPS, and respond with prominent induction of proinflammatory cytokines, only media from Ep cultures subjected to high-dose PDT showed stimulatory activity. In contrast to Fb (Figure 1E), macrophages did not measurably respond to IL-1 by enhanced IL-6 production (Figure 2G and data not shown).

Malignant transformation changes expression and PDT-dependent release of FSA

To evaluate basal expression and PDT-dependent increase of FSA by primary lung Ep, as well as the impact of malignant transformation on these properties, Ep from bronchial section (BEC), peripheral portions of non-tumour-involved lung specimen (N-Ep) and from tumours (T-Ep) were analysed. A 50-nM HPPH-PDT dose was used because it is predicted to yield maximal FSA release over the subsequent 24 h. While there was a large range of basal FSA release among cell preparations, a $\sim$10-fold maximal increase by PDT was determined for all N-Ep and most T-Ep (Figure 2H). There was no significant difference in FSA release by cells subjected to equally effective PDT through mitochondrially localised HPPH or lysosomally localised HPPH-Gal. Among 21 cases of lung tumours, two adenocarcinoma cases (L297 and L299) were exceptions in that they showed a $\sim$50-fold elevated basal FSA activity that was further enhanced by PDT (Figure 2H).

While all N-Ep and most T-Ep cultures have limited expansion (3–7 passages), some cases maintain proliferative activity for extended passages. These cultures generally retained FSA production and PDT-inducible release, albeit at lower level compared with normal cells (Figure 2I). One line (L301) proved to be devoid of FSA and was comparable to the established lung cell line A549.

To assess PDT-mediated changes in Ep at the level of transcripts, BEC cultures were subjected to 25 nM HPPH-PDT ($\sim$50% cell death), leaving sufficient surviving cells for detecting inducible genes. RNAs extracted 2 and 24 h post PDT were subjected to an Affymetrix genechip array. In close agreement with previous reports regarding other cell types (Buytaert *et al*, 2008; Sanovic *et al*, 2009; Kammerer *et al*, 2011), the major transcript changes were determined for genes encoding stress response with a striking minimal alteration for cytokines and chemokines associated with tissue damage (Supplementary Table 1). A three-fold increase was detected for IL-6, but the relative expression level of IL-6 remained low, not yielding biologically effective cytokine concentrations as determined by the lack of STAT3 phosphorylation in Fb (Figure 1A) or by a nonsignificant induction of GFP in the H-35 cell assay (data not shown). Treatment of Ep with actinomycin D or cycloheximide before PDT did not measurably lower the release of FSA (data not shown) suggesting that FSA constitutes preformed alarmins.

PDT dose- and time-dependent release of FSA and DAMPs

The kinetics by which FSA (Figure 3A) and DAMPs (Figure 3B) were released by Ep following PDT indicated that the appearance FSA and cellular constituents in the medium temporally coincided to 50–100 nM HPPH-PDT. At lower PDT doses (e.g., mediated by 25 nM HPPH, Figure 3A and B) that promoted apoptotic cell death, we consistently observed that the release of FSA was temporally delayed with higher amounts recovered several hours post PDT. In contrast, at higher PDT doses and despite the progressively enhanced immediate cell killing, the recovery of FSA was reduced relative to DAMPs. Based on $>$50 separate analyses, the optimal recovery of FSA was determined following PDT with 50–100 nM HPPH that yielded roughly equal amounts of FSA released within the first 2 h post PDT and the subsequent 22 h.

Major bioactive component of FSA is IL-1α

To assess the molecular complexity of FSA, conditioned Ep media were size-fractionated under physiological conditions on a Sephadex G150 column (Figure 4). Fb-stimulatory activity from cells without PDT eluted predominantly with $\sim$17 kD (Figure 4B). Medium collected 2 h after PDT showed enhanced activity at the 17-kD position with additional activity at $\sim$35 kD. Medium collected 2–24 h post PDT had further enhanced FSA activities at 17 and 35 kD and minor activities at $\sim$50 and $\sim$100 kD. Western blot analyses indicated an overlap of cytochrome C with 17 kD FSA, whereas PRX1 and HMGB1 in part co-eluted with FSA at 50 kD and higher (Figure 4A, upper panel). Elution of HMGB1, as with actin and PRX1, at an apparent molecular size larger than found for the denatured and reduced protein, suggested association with complexes that did not disaggregate under physiological salt and pH conditions. Chromatography of recombinant IL-1β yielded a single activity peak at 17 kD (data not shown) and COS-1 cell-derived IL-1α eluted with the major activity at 17 kD and second portion at $\sim$35 kD (Figure 4B). The elution of IL-1α activity coincided with that of IL-1α protein in Ep homogenate (Figure 4A, lower panel) and is in agreement with the properties reported for the pro-form and proteolytically processed IL-1α (Moussion *et al*, 2008; Gross *et al*, 2012).

The size profile for FSA as determined by the induced IL-6 production (Figure 4B), was similar to that for enhanced neutrophil binding (Figure 4C). This concordance suggests that both responses are determined by the same set of mediators of which IL-1 isoforms appear to be involved. Signalling analyses (Figure 1B and D) have demonstrated the ability of Fb to respond to IL-1α and IL-1β, but not to the related forms IL-1F9 (IL-36γ) and IL-33.

The relative contribution of IL-1α and IL-1β to FSA was determined by antibody-mediated neutralization of signalling (Figure 5A), increased production of IL-6 (Figure 5B) and enhanced neutrophil binding (Figure 5C). The data indicated that FSA released by non-PDT-treated Ep is primarily composed of IL-1β and IL-1α. The elevated basal level of FSA observed for certain preparations of T-Ep cultures (L297 and L299; Figure 3A) was mainly attributable to a higher concentration of IL-1β (data not shown). PDT caused the release of intracellular IL-1α accounting largely for FSA detectable in non-fractionated CM as well as the size-separated fraction (Figure 5A). In line with the predicted mode of IL-1α's alarmin function (Dinarello, 2009; Cohen *et al*, 2010), PDT-dependent cell damage mobilised the release of this IL-1 from a pre-existing intracellular pool. The amount of biologically active IL-1 in intact Ep cultures was confirmed by the analysis of whole-cell homogenate (Figures 4A and 5A). Quantification of immunoblot signals indicated that the combined antibody-dependent neutralization of IL-1α and IL-1β reduced Ep-derived FSA by 80–95%.

Ep-derived FSA activates a proinflammatory programme in Fb

As PDT-dependent tissue damage is an effective activator of local inflammation, we determined the profile of gene regulation by

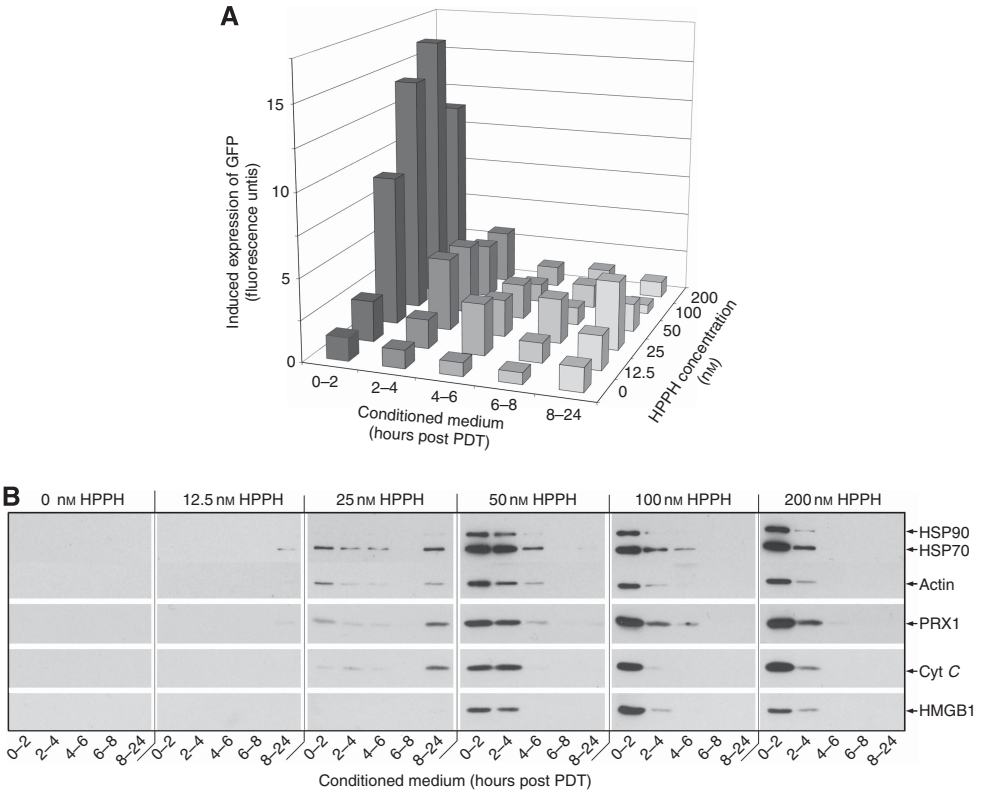

Figure 3 Kinetics of FSA and DAMP release by PDT-treated T-Ep. Adenocarcinoma-derived T-Ep, passage 4, in a 6-well plate was treated with the indicated concentrations of HPPH for 30 min followed by a 24-h culture period. After light treatment, the cultures were incubated for additional 24 h with periodic collection of CM and replacement with fresh media. Aliquots of the culture media were three-fold diluted, used to determine FSA by treating N-Fb for 24 h and determining the IL-6-dependent induction of GFP in H-35 cells (**A**). Equal aliquots of Ep-conditioned media were analysed for the indicated proteins by western blotting (**B**).

Ep-derived FSA in Fb. Transcripts isolated after 24 h treatment were analysed by Affymetrix genechip array (Table 1). Three separate assays yielded highly consistent patterns that bore the signature of IL-1-type proinflammatory mediators (Nowinski *et al*, 2004; Taberner *et al*, 2005). The list of inducible genes indicated a particularly high induction of several CXC chemokines, which, along with ICAM-1 induction, correlates with the prominent neutrophil binding of treated Fb (Figure 1C). The increase of IL-6-type cytokines (IL-6, IL-11 and LIF) is in line with the bioactivity reported by the H-35 cell assay (Figure 2F). No appreciable induction of IL-1α or IL-1β was determined, whereas the related family member IL-33 was several fold increased. As Fb did not respond to IL-33 (Figure 1D), an autocrine action was excluded.

Subcellular site of PDT dictates release of FSA and cell death

The studies thus far used mitochondrially localised HPPH. Plasma membrane-confined and lysosomally localised PSs are two additional PDT options (Zheng *et al*, 2009; Mitsunaga *et al*, 2011; Tracy *et al*, 2011). To determine the impact of the photoreaction at these sites, HPPH-Gal was applied. 2-(1-Hexyloxyethyl)-2-devinylpyropheophorbide-a-Gal binds to the plasma membrane, is endocytosed and accumulates in lysosomes (Figure 6A). To limit the photoreaction to the cell surface, HPPH-Gal binding and light treatment were carried out on ice. The photoreaction at the plasma membrane and lysosomes resulted in an oxidative crosslinking of STAT3 and loss of EGFR that was proportional to the amount of cell-associated PS (Figure 6B and C). The PS dose–effect relationship was comparable to that determined for HPPH-PDT (Figure 2B). However, the surface photoreaction proved to be $\sim$10-fold more effective in cell killing than the lysosomal reaction (Figure 6B), the latter being comparable to that of mitochondrial PDT (Figure 2B). Fb-stimulatory activity release (Figure 6D) correlated with cell death and the appearance of cellular proteins in the culture supernatant (Figure 6E). Of note is that despite the immediate lethal response to HPPH-Gal PDT, externalisation of cellular proteins was not instantaneous, but occurred over several hours. Moreover, and confirmed in three independent experimental series, surface PDT did not result in the detectable release of cytochrome C, whereas lysosomal, like mitochondrial, PDT yielded cytochrome C release (Figure 6E). Recovery of FSA from cells subjected to lysosomal PDT, as with mitochondrial PDT, peaked with the dose at which close to 100% cell death was reached (Figure 6D). At higher PDT doses, recovery of FSA in the culture medium was lower.

Intracellular, but not extracellular, PDT inactivates cellular alarmins

The identification of IL-1α as the major alarmin of Ep exposed to lethal PDT (Figure 5) suggested that cell-associated IL-1 activity preexisted and no PDT-induced expression was required (Supplementary Table 1). The amount of IL-1 in Ep cultures was determined by testing cell-free homogenates and corresponding conditioned media to stimulate, in a dose-dependent manner, IL-6 expression in Fb (Figure 6F and G). The concentrations measured by the bioassay could be confirmed for selected samples by quantitation of the cytokine proteins with the Luminex immune bead assay (data not shown). Two distinct PDT modes were evaluated: intracellular HPPH-PDT and cell surface HPPH-Gal-PDT. The accumulation of HPPH in mitochondria was

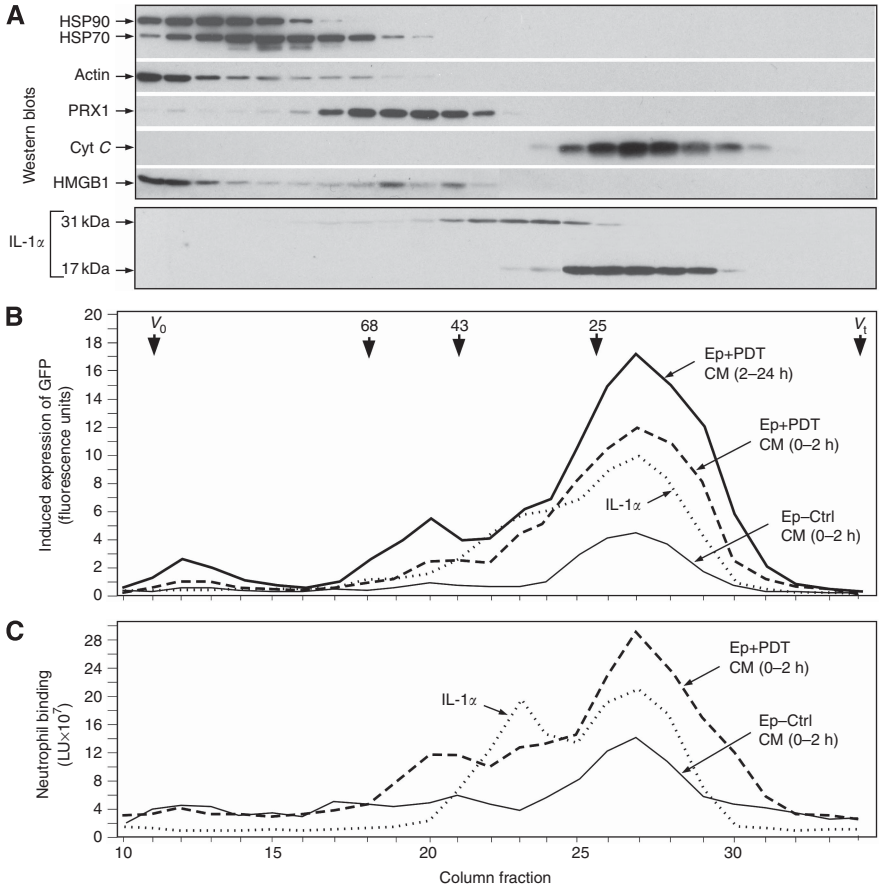

Figure 4 Size separation of proteins in CM of PDT-treated T-Ep. Duplicate cultures of T-Ep, passage 3, in a 10-cm-diameter culture dish were treated either as light control or with 25 nM HPPH-PDT. Conditioned medium 2 and 24 h post PDT were concentrated and subjected to chromatography on a G-150 Sephadex column. Proteins in each fraction were analysed for the indicated proteins (**A,** upper panel), FSA in the coupled Fb-H-35 cell assay (**B**) and for induced neutrophil binding to the treated Fb (**C**). Detection of the FSA activity by chromatographed COS-1 cell-derived IL-1α is included in (**B** and **C**). The centrifuged homogenate of untreated T-Ep from one 10-cm dish was similarly size fractionated and the entire fractions were analysed for IL-1α protein by western blotting (**A,** lower panel). The elution positions of the molecular size markers (in kDa) are indicated at the top of the column elution profile.

proportional to the concentration of HPPH added to the culture medium (Supplementary Figure 1A). In contrast, HPPH-Gal binding to the cell surface was limited by saturation of extracellular binding sites that occurred at ~1000 nM HPPH-Gal (Supplementary Figure 1E). In both settings, however, the amounts of cell-associated PS at the highest concentrations were in several-fold excess to that necessary for 100% lethal PDT.

An HPPH-PDT dose-dependent loss of cell-associated FSA was detectable and reached zero at the highest PDT dose (Figure 6F). The loss of FSA from the cellular fraction at a lower PDT dose correlated with the appearance of FSA in the culture supernatant with a maximum at ~50 nM HPPH. At higher PDT dose, FSA in the culture medium decreased to zero, indicating a complete inactivation of cellular FSA/IL-1 activity in HPPH-PDT-treated culture.

A different outcome was determined for Ep subjected to cell surface PDT. All cells were killed at the lowest HPPH-Gal concentration (Supplementary Figure 1E) and that was accompanied by a depletion of FSA from the cellular material (Figure 6G). Essentially all cell-associated FSA could be recovered in the CM irrespective of the level of PDT. At high HPPH-Gal-PDT doses, the cellular remnants were fixed to the support as seen for HPPH-treated cells, but differed in that all nuclei show a marked vacuolar structure (Supplementary Figure 1D and F). Taken together, these results indicate that the mode of PDT determines not only the level of cell stress and lethal progression, but also the presentation of alarmins.

DISCUSSION

This study revealed that PDT is not only effective in killing target Ep, but also potently simulates stromal Fb, and surprisingly to a much lower extent macrophages, to express proinflammatory mediators. This property reflects the combined action of all alarmins released by the PDT-damaged cells and is considered to be relevant for initiating inflammation at the site of PDT *in vivo*. Hallmarks of this process are the induced expression of CXC chemokines, enhanced cell surface presentation of ICAM-1 and increased neutrophil binding. Recruitment of neutrophils and their local retention in turn assist in the delivery of heightened inflammatory cues by neutrophil-derived mediators and extracellular enzyme activities (Chalaris *et al*, 2007; Bratton and Henson, 2011; Lefrancais *et al*, 2012). Unlike mechanical cell damage that similarly triggers local inflammation that is proportional to the extent of cell damage, the response to PDT incorporates a PDT type- and dose-dependence that leads to Fb stimulation that is not strictly proportional to the magnitude of photoreaction. Hence, by selecting PDT conditions that involve site-specific delivery of PS and intensity of photoreaction, the level of the local inflammatory response can be predetermined. The dose dependence of the PDT-induced inflammatory reaction and subsequent systemic acute phase responses *in vivo* has been observed earlier (Gollnick *et al*, 2003; Henderson *et al*, 2006; Kousis *et al*, 2007; Seshadri *et al*, 2008). Here, we report an in-depth examination of the mechanisms involved.

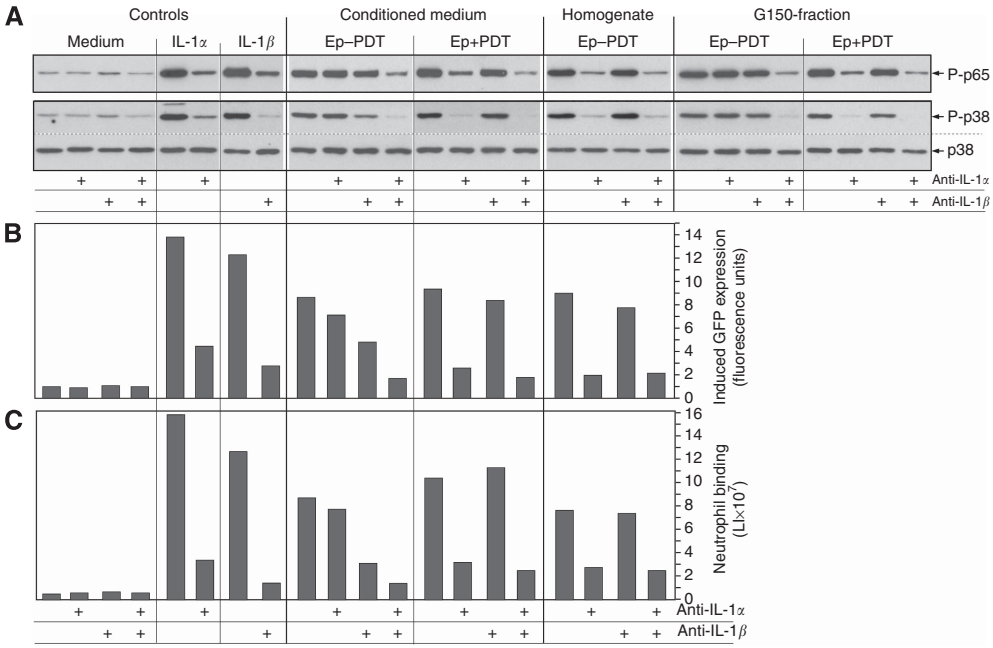

Figure 5 Identification of IL-1α and IL-1β as Ep-derived FSA and alarmin. Conditioned medium of control Ep cultures (*Ep-PDT*) and PDT-treaded Ep cultures (*Ep + PDT*), whole-cell homogenate of control Ep and Sephadex G-150-purified 17 kD FSA were reacted with antibodies against IL-1α or IL-1β as indicated and then tested for the ability to activate signalling (**A**), to enhance IL-6 that induces GFP expression in H-35 cells (**B**) and to increase neutrophil binding (**C**).

The principal alarmin in the Ep model is IL-1α, which is particularly effective on Fb. The prominence of IL-1α as an Ep alarmin is in accordance with previous reports (Dinarello, 2009; Cohen *et al*, 2010). While resident tissue macrophages function as the primary guards against pathogens and respond to these by massive release of inflammatory mediators (Laskin *et al*, 2011), these cells do not appear to recognise PDT-damaged Ep-derived alarmins as effective stimulants. Moreover, while DAMPs have been found to exert alarmin functions (Bianchi, 2007), our assays could not assign an appreciable activity to these. The quantitative assessment of the Fb response to IL-1- or Ep-derived alarmins indicated an induction and secretion of cytokines, such as IL-6, which approached that of endotoxin-activated macrophages (Figure 1E and 2F-I). While the photoreaction in target cells is highly effective in eliciting oxidative reactions that induce transcription of stress response (Buytaert *et al*, 2008; Kammerer *et al*, 2011), the PDT-regulated expression of IL-6 and related cytokines by Ep appears to be functionally inconsequential. Considering the abundance of stromal cells in lung and tumour tissue, the local presentation of inflammatory mediators through Fbs alone will be appreciable. High-level production of IL-6 by non-hematopoietic cells at sites of PDT-mediated tissue damage has been implicated to contribute to systemic distribution and activation of acute phase responses at distal organ sites (Gollnick *et al*, 2003; Kousis *et al*, 2007).

Kinetic studies of DAMP and IL-1 release indicated that even upon lethal light treatment with internalised PS, alarmins are not immediately released. Fb-stimulatory/IL-1 activity leaks into the extracellular milieu over several hours (Figure 3). At extremely high PDT doses, IL-1 activity was reduced, possibly through direct inactivation by oxidative reactions and/or degradation through intracellular proteases, or its release obstructed by the oxidative crosslinking of cellular structures. Photodynamic therapy mediated by cell surface-bound PS is highly lethal and facilitates the release of intracellular material, including alarmins. Moreover, while oxidative reactions propagate into the intracellular compartments, accounting for STAT3 crosslinking (Figure 6C), these reactions, together with any degrading activities, are ineffective in inactivating IL-1 (Figure 6F). Hence, we predict that surface-directed PSs, which often are present at lower concentrations on target cells than internalised PS (Mitsunaga *et al*, 2011), would still be able to achieve lethal action and would mobilise a prominent Fb response.

PDT-stimulated inflammation aids tumour control through the recruitment of immune cells to the treatment site, enhanced antigen uptake and processing by dendritic cells and phagocytes, and development of antitumour effector function by lymphocytes (Gollnick *et al*, 2002; Kousis *et al*, 2007; Agostinis *et al*, 2011). Neutrophils retained by Fb (Figure 1) and endothelial cells (data not presented) add their mediators to the local milieu. The prominent production of IL-6 by Fb may assist in the stimulation of DCs and recruitment of lymphocytes through trans-signalling enabled by soluble IL-6 receptor-alpha released by neutrophils (Chalaris *et al*, 2007) and probably Ep as well. Some tumour cells intrinsically determine the level of stromal cell activation and inflammation by the basal expression level of IL-1α and IL-1β. Tumours with several-fold elevated expression of IL-1, as seen for two adenocarcinoma-derived cell cultures (Figure 2H), may magnify the Fb response and inflammation. In tumour cells with a loss of IL-1 expression, such as A549, the inflammatory response should be subdued, and dependent on alarmins derived from collateral damage to the treated tissue. The earlier preclinical observation (Henderson *et al*, 2006; Seshadri *et al*, 2008) that high-dose PDT was capable to cause extensive tumour necrosis but a relatively low inflammatory tissue reaction can now be explained, in part, through the PDT-mediated inactivation of alarmins.

Contrary to the beneficial role of inflammation, it also needs to be considered that an inflammatory environment and innate immune cells contribute paracrine factors that assist in tumour cell survival via activation of the NFkB pathway and enhance proliferation via growth factors and cytokines (Sims *et al*, 2010; Kuraishy *et al*, 2011; DiDonato *et al*, 2012). Hence, inflammation may not only assist in tumorigenic processes (Stathopoulos *et al*, 2007; Meylan *et al*, 2009; Sunaga *et al*, 2012) but also exert

Table 1 Genes inducible by Ep-derived alarmins in normal pulmonary fibroblasts

Probeset ID	Gene title	Gene symbol	Exp 1		Exp 2		Exp 3	
			Expr.	Fold	Expr.	Fold	Expr.	Fold
Chemokines								
211506_s_at	Interleukin 8	IL8	19376	196.7	23217	239.9	32161	345.9
204470_at	Chemokine (C–X–C motif) ligand 1	CXCL1	42127	49.5	35994	42.9	43967	53.3
209774_x_at	Chemokine (C–X–C motif) ligand 2	CXCL2	13412	114.6	10028	91.3	15510	132.3
207850_at	Chemokine (C–X–C motif) ligand 3	CXCL3	15600	102.7	17404	101.5	18297	114.1
215101_s_at	Chemokine (C–X–C motif) ligand 5	CXCL5	5704	126.6	9875	220.7	15560	341.3
206336_at	Chemokine (C–X–C motif) ligand 6	CXCL6	18145	20.4	12643	13.4	16653	19.0
216598_s_at	Chemokine (C–C motif) ligand 2	CCL2	34846	4.3	34068	4.4	31626	4.0
208075_s_at	Chemokine (C–C motif) ligand 7	CCL7	3903	14.9	3449	13.9	1904	7.2
214038_at	Chemokine (C–C motif) ligand 8	CCL8	1106	8.6	1192	11.7	750	6.6
210133_at	Chemokine (C–C motif) ligand 11	CCL11	780	3.4	1294	5.8	604	1.8
206407_s_at	Chemokine (C–C motif) ligand 13	CCL13	352	2.5	591	5.1	303	2.2
205476_at	Chemokine (C–C motif) ligand 20	CCL20	526	8.8	940	17.2	1680	30.7
Cytokines								
205207_at	Interleukin 6	IL6	32180	24.2	29455	23.8	36264	28.2
206924_at	Interleukin 11	IL11	310	3.7	1737	19.4	1178	11.0
205266_at	Leukaemia inhibitory factor	LIF	1631	6.0	1218	5.1	1111	4.3
206569_at	Interleukin 24	IL24	850	7.5	1099	8.9	1126	10.0
203828_s_at	Interleukin 32	IL32	2697	10.3	991	3.7	2566	10.1
209821_at	Interleukin 33	IL33	621	12.2	851	17.2	834	18.0
Growth factors and related								
213921_at	Somatostatin	SST	2176	7.0	17922	67.8	5757	18.6
205767_at	Epiregulin	EREG	786	8.3	1685	18.3	495	5.2
205239_at	Amphiregulin	AREG	3204	4.6	9003	13.1	1343	2.0
243296_at	Pre-B-cell colony-enhancing factor 1	PBEF1	2456	11.5	2777	12.9	1991	9.3
202410_x_at	Insulin-like growth factor 2	IGF2	976	4.9	489	2.2	1123	5.3
204422_s_at	Fibroblast growth factor 2 (basic)	FGF2	9988	3.2	12919	4.4	11995	3.9
222802_at	Endothelin 1	EDN1	847	3.2	1501	6.2	1130	3.5
205290_s_at	Bone morphogenetic protein 2	BMP2	619	3.0	788	4.6	678	3.5
210229_s_at	Colony-stimulating factor 2 (granulocyte-macrophage)	CSF2	544	5.6	152	1.0	1357	14.7
202510_s_at	Tumour necrosis factor, alpha-induced protein 2	TNFAIP2	3416	4.7	2956	4.7	3079	4.5
202643_s_at	Tumour necrosis factor, alpha-induced protein 3	TNFAIP3	2596	34.3	1907	22.6	2775	32.5
206025_s_at	Tumour necrosis factor, alpha-induced protein 6	TNFAIP6	18571	10.7	22814	12.9	19994	11.1
202357_s_at	Complement factor B	CFB	938	12.6	229	2.0	513	7.3
Proteases								
204475_at	Matrix metallopeptidase 1 (interstitial collagenase)	MMP1	24670	4.2	11180	1.8	31020	5.5
205680_at	Matrix metallopeptidase 10 (stromelysin 2)	MMP10	546	2.4	280	1.2	680	4.1
204580_at	Matrix metallopeptidase 12 (macrophage elastase)	MMP12	3597	8.9	331	-1.3	4716	12.8
224942_at	Pregnancy-associated plasma protein A, pappalysin 1	PAPPA	6121	15.4	6342	16.5	4159	10.6
202902_s_at	Cathepsin S	CTSS	916	5.7	495	3.1	1232	7.9
Redox-related								
215223_s_at	Superoxide dismutase 2, mitochondrial	SOD2	24302	34.2	19873	24.8	30852	41.9
210367_s_at	Prostaglandin E synthase	PTGES	6402	14.4	9601	19.5	7756	16.1
204748_at	Prostaglandin-endoperoxide synthase 2 (COX-2)	PTGS2	1294	8.5	1375	10.7	1433	10.7
Receptors and signalling								
202636 _at	Intercellular adhesion molecule 1 (CD54)	ICAM1	1719	17.6	1907	11.6	2134	22.0
204273_at	Endothelin receptor-type B	EDNRB	3095	8.2	5719	14.8	3050	8.7
205729_at	Oncostatin M receptor	OSMR	1235	3.0	1579	3.8	1823	4.8
206172_at	Interleukin 13 receptor, alpha 2	IL13RA2	8089	4.2	13358	6.8	11928	5.7
212657_s_at	Interleukin 1 receptor antagonist	IL1RN	263	3.2	345	3.8	218	2.4
231779_at	Interleukin-1 receptor-associated kinase 2	IRAK2	1096	4.3	1282	4.5	1249	4.4
218353_at	Regulator of G-protein signalling 5	RGS5	825	6.2	544	5.4	781	5.9
223809_at	Regulator of G-protein signalling 18	RGS18	388	4.8	1609	15.0	678	7.0

Abbreviations: Ep = epithelial cell; Exp = experiment; Expr. = expression. In three independent experiments, pairs of N-Fb cultures were treated for 24 h with medium alone or containing 1/10 diluted 24-h-conditioned medium from BEC subjected to 50 nM HPPH-PDT. Transcripts were analysed by Affymetrix array and compared with control cultures for genes induced at least four-fold in one of the sets.

supporting activities towards established tumours by aiding in the recovery of sub-lethally damaged tumour cells. Of note is that PDT causes fundamental changes to membrane receptor systems and the signal-transducing capabilities of the target cells, some of which are associated with growth suppression (e.g., by OSM) or growth stimulation (e.g., by EGF) of Ep (Wong *et al*, 2003; Liu *et al*, 2004). The restoration of pretreatment regulatory capability of PDT-surviving cells appears to be a slow process that can take up

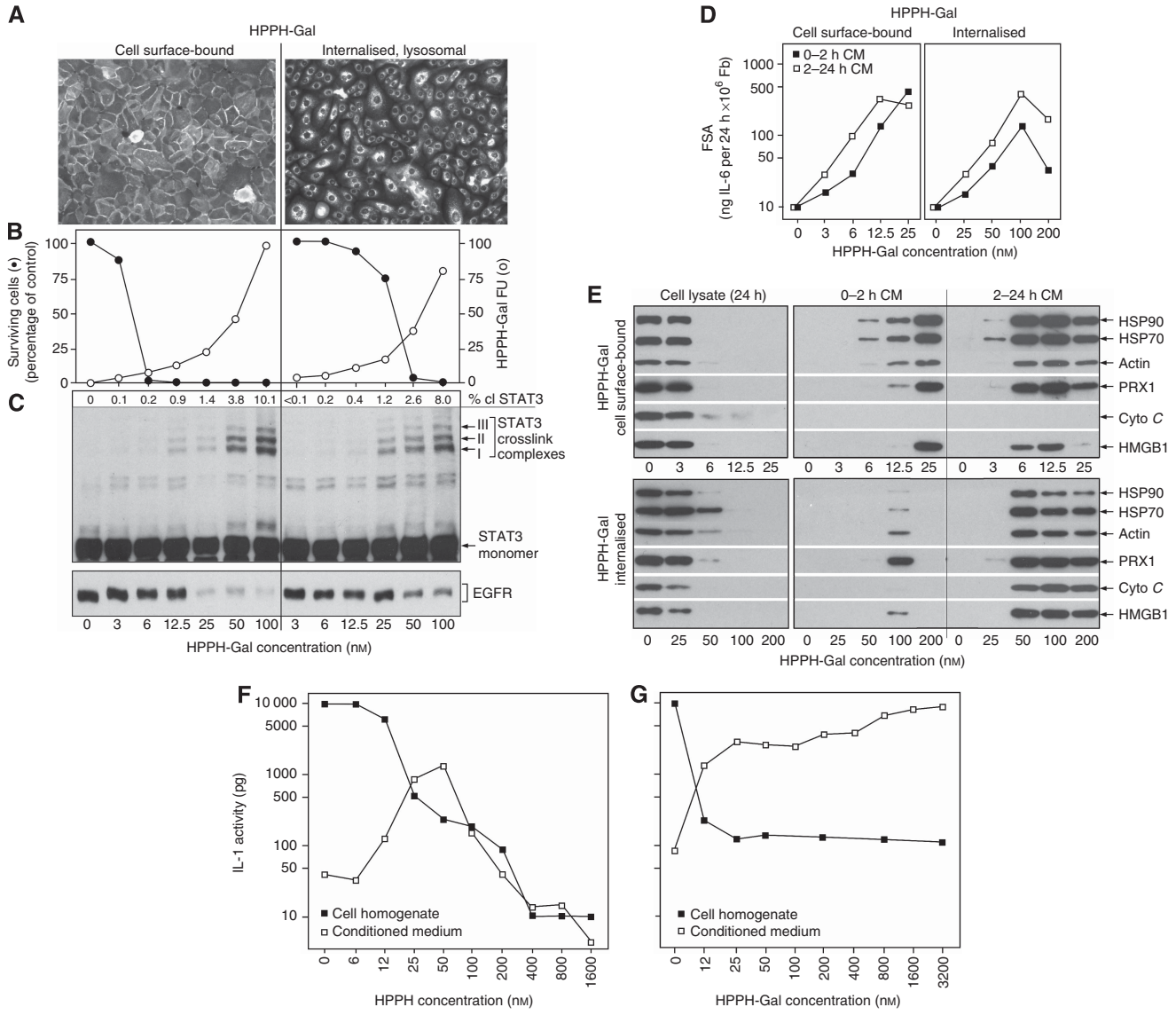

Figure 6 Enhanced cell damage and release of FSA by cell surface-restricted photoreaction. **A**, 100 nM HPPH-Gal was bound to the cell surface of T-Ep, passage 3, during 30-min incubation at 4° C followed by internalisation and lysosomal deposition during a 24-h incubation at 37° C. Fluorescent micrographs of the cultures at × 100 magnification are shown. (**B, C)** Replicate sets T-Ep cultures in 6-well dishes were reacted with the indicated concentrations of HPPH-Gal restricted to cell surface or to be internalised. The cell-associated fluorescence was quantified (**B**, open circles) and the cells in all sets were treated on ice with 665 nm light. One set of cultures was immediately lysed and analysed by western blotting to the extent of STAT3 crosslinking and loss of EGFR (**C**). The other set was cultured for an additional 24 h to determine survival rate (**B**, closed circle). (**D**, **E**) Duplicate set of T-Ep, passage 5, were subjected to HPPH-Gal binding to cell surface or lysosomal accumulation at the indicated HPPH-Gal dose. The photoreaction was carried out at 0° C and the cultures were incubated for an additional 24 h. Conditioned media collected after 2 h and 24 h were analysed for FSA on N-Fb cultures (**D**). Equivalent aliquots of cell lysates and conditioned media were analysed by western blotting for the indicated DAMPs (**E**). (**F**, **G**) Replicate cultures of T-Ep in 6-well plates were subjected to high-dose mitochondrial HPPH-PDT (**F**) or cell-surface HPPH-Gal PDT (**G**) with light treatment carried out on ice. After 4-h post-PDT incubation, the adherent cells, combined with cellular debris recovered by centrifugation of CM, were homogenised. Aliquots of the cell homogenates and cell-free-CM were analysed for the amount of IL-1 activity per culture.

to several days. Moreover, tissue damage owing to PDT inevitably stimulates the process of wound healing that involves enhanced local expression of growth-supporting extracellular matrix, presentation of growth factors, revascularization, diminished hypoxia, and enhanced influx of nutrients and metabolites. Not only stromal cells, but PDT-surviving epithelial tumour cells as well, benefit from the growth-favoring action of inflammation and post-inflammatory reactions. As suggested by our finding, the precise combination of alarmin-expression status of the tumour, level of PS loading, intensity and duration of photoreaction, degree of tissue damage, composition of PDT-surviving cell population and profile of induced inflammatory reactions by resident and infiltrating cells are relevant determinants of the outcome of tumour PDT. The PDT-mediated mobilisation of alarmins has a central role in initiating this complex circuitry. Specific recommendation regarding the application of our findings to clinical PDT awaits the definition of the precise anti- and pro-tumour activities exerted by the alarmin-mobilised inflammation and immune cells functions. While a robust acute inflammatory reaction at the PDT-treated tumour sites with optimal preservation and release of alarmins may offer the best condition for a favourable anti-tumour immune response (Agostinis *et al*, 2011), the effectiveness of the inflammatory milieu onto the PDT-surviving tumour cells is still an unknown element.

ACKNOWLEDGEMENTS

We thank Dr Ravendra Pandey and Joseph Missert for preparations of PSs, the members of the Department of Pathology and Tissue Procurement Services at RPCI, headed by Drs Richard Cheney and Carl Morrison, for surgical lung tissue, Dr Meir Wetzler and the Bone Marrow Procurement team for human neutrophil preparations, the laser core of the PDT Centre for assistance in laser application, and the Gene Expression Core for Affymetrix array and data analysis, and Dr Jihnhee Yu, Department of Biostatistics, SUNY at Buffalo, for box plot presentation of data. This research was supported by NCI grants P01CA55791, Grant of the Roswell Park Alliance and RPCI Support Grant P30CA16056.

Supplementary Information accompanies the paper on British Journal of Cancer website (http://www.nature.com/bjc)

REFERENCES

Agostinis P, Berg K, Cengel KA, Foster TH, Girotti AW, Gollnick SO, Hahn SM, Hamblin MR, Juzeniene A, Kessel D, Korbelik M, Moan J, Mroz P, Nowis D, Piette J, Wilson BC, Golab J (2011) Photodynamic therapy of cancer: an update. *CA Cancer J Clin* **61**(4): 250–281

Baumann H, Gauldie J (1994) The acute phase response. *Immunol Today* **15**(2): 74–80

Baumann H, Prowse KR, Marinkovic S, Won KA, Jahreis GP (1989) Stimulation of hepatic acute phase response by cytokines and glucocorticoids. *Ann N Y Acad Sci* **557**: 280–295; discussion 295–296

Bianchi ME (2007) DAMPs, PAMPs and alarmins: all we need to know about danger. *J Leukoc Biol* **81**(1): 1–5

Bratton DL, Henson PM (2011) Neutrophil clearance: when the party is over, clean-up begins. *Trends Immunol* **32**(8): 350–357

Bryant C, Fitzgerald KA (2009) Molecular mechanisms involved in inflammasome activation. *Trends Cell Biol* **19**(9): 455–464

Buytaert E, Dewaele M, Agostinis P (2007) Molecular effectors of multiple cell death pathways initiated by photodynamic therapy. *Biochim Biophys Acta* **1776**(1): 86–107

Buytaert E, Matroule JY, Durinck S, Close P, Kocanova S, Vandenheede JR, de Witte PA, Piette J, Agostinis P (2008) Molecular effectors and modulators of hypericin-mediated cell death in bladder cancer cells. *Oncogene* **27**(13): 1916–1929

Chalaris A, Rabe B, Paliga K, Lange H, Laskay T, Fielding CA, Jones SA, Rose-John S, Scheller J (2007) Apoptosis is a natural stimulus of IL6R shedding and contributes to the proinflammatory trans-signaling function of neutrophils. *Blood* **110**(6): 1748–1755

Chattopadhyay S, Tracy E, Liang P, Robledo O, Rose-John S, Baumann H (2007) Interleukin-31 and oncostatin-M mediate distinct signaling reactions and response patterns in lung epithelial cells. *J Biol Chem* **282**(5): 3014–3026

Cohen I, Rider P, Carmi Y, Braiman A, Dotan S, White MR, Voronov E, Martin MU, Dinarello CA, Apte RN (2010) Differential release of chromatin-bound IL-1alpha discriminates between necrotic and apoptotic cell death by the ability to induce sterile inflammation. *Proc Natl Acad Sci USA* **107**(6): 2574–2579

DiDonato JA, Mercurio F, Karin M (2012) NF-kappaB and the link between inflammation and cancer. *Immunol Rev* **246**(1): 379–400

Dinarello CA (2009) Immunological and inflammatory functions of the interleukin-1 family. *Annu Rev Immunol* **27**: 519–550

Foell D, Wittkowski H, Vogl T, Roth J (2007) S100 proteins expressed in phagocytes: a novel group of damage-associated molecular pattern molecules. *J Leukoc Biol* **81**(1): 28–37

Gallucci S, Matzinger P (2001) Danger signals: SOS to the immune system. *Curr Opin Immunol* **13**(1): 114–119

Garg AD, Krysko DV, Vandenabeele P, Agostinis P (2011) DAMPs and PDT-mediated photo-oxidative stress: exploring the unknown. *Photochem Photobiol Sci* **10**(5): 670–680

Gollnick SO, Evans SS, Baumann H, Owczarczak B, Maier P, Vaughan L, Wang WC, Unger E, Henderson BW (2003) Role of cytokines in photodynamic therapy-induced local and systemic inflammation. *Br J Cancer* **88**(11): 1772–1779

Gollnick SO, Vaughan L, Henderson BW (2002) Generation of effective antitumor vaccines using photodynamic therapy. *Cancer Res* **62**(6): 1604–1608

Gross O, Yazdi AS, Thomas CJ, Masin M, Heinz LX, Guarda G, Quadroni M, Drexler SK, Tschopp J (2012) Inflammasome activators induce interleukin-1alpha secretion via distinct pathways with differential requirement for the protease function of caspase-1. *Immunity* **36**(3): 388–400

Hawthorn L, Stein L, Panzarella J, Loewen GM, Baumann H (2006) Characterization of cell-type specific profiles in tissues and isolated cells from squamous cell carcinomas of the lung. *Lung Cancer* **53**(2): 129–142

Henderson BW, Busch TM, Snyder JW (2006) Fluence rate as a modulator of PDT mechanisms. *Lasers Surg Med* **38**(5): 489–493

Henderson BW, Daroqui C, Tracy E, Vaughan LA, Loewen GM, Cooper MT, Baumann H (2007) Cross-linking of signal transducer and activator of transcription 3–a molecular marker for the photodynamic reaction in cells and tumors. *Clin Cancer Res* **13**(11): 3156–3163

Immenschuh S, Song DX, Satoh H, Muller-Eberhard U (1995) The type II hemopexin interleukin-6 response element predominates the transcriptional regulation of the hemopexin acute phase responsiveness. *Biochem Biophys Res Commun* **207**(1): 202–208

Kammerer R, Buchner A, Palluch P, Pongratz T, Oboukhovskij K, Beyer W, Johansson A, Stepp H, Baumgartner R, Zimmermann W (2011) Induction of immune mediators in glioma and prostate cancer cells by non-lethal photodynamic therapy. *PLoS One* **6**(6): e21834

Kousis PC, Henderson BW, Maier PG, Gollnick SO (2007) Photodynamic therapy enhancement of antitumor immunity is regulated by neutrophils. *Cancer Res* **67**(21): 10501–10510

Kuraishy A, Karin M, Grivennikov SI (2011) Tumor promotion via injury- and death-induced inflammation. *Immunity* **35**(4): 467–477

Laskin DL, Sunil VR, Gardner CR, Laskin JD (2011) Macrophages and tissue injury: agents of defense or destruction? *Annu Rev Pharmacol Toxicol* **51**: 267–288

Lefrancais E, Roga S, Gautier V, Gonzalez-de-Peredo A, Monsarrat B, Girard JP, Cayrol C (2012) IL-33 is processed into mature bioactive forms by neutrophil elastase and cathepsin G. *Proc Natl Acad Sci USA* **109**(5): 1673–1678

Liu W, Oseroff AR, Baumann H (2004) Photodynamic therapy causes cross-linking of signal transducer and activator of transcription proteins and attenuation of interleukin-6 cytokine responsiveness in epithelial cells. *Cancer Res* **64**(18): 6579–6587

Loewen GM, Tracy E, Blanchard F, Tan D, Yu J, Raza S, Matsui S, Baumann H (2005) Transformation of human bronchial epithelial cells alters responsiveness to inflammatory cytokines. *BMC Cancer* **5**: 145

Lotze MT, Zeh HJ, Rubartelli A, Sparvero LJ, Amoscato AA, Washburn NR, Devera ME, Liang X, Tor M, Billiar T (2007) The grateful dead: damage-associated molecular pattern molecules and reduction/oxidation regulate immunity. *Immunol Rev* **220**: 60–81

Meylan E, Dooley AL, Feldser DM, Shen L, Turk E, Ouyang C, Jacks T (2009) Requirement for NF-kappaB signalling in a mouse model of lung adenocarcinoma. *Nature* **462**(7269): 104–107

Mitsunaga M, Ogawa M, Kosaka N, Rosenblum LT, Choyke PL, Kobayashi H (2011) Cancer cell-selective *in vivo* near infrared photoimmunotherapy targeting specific membrane molecules. *Nat Med* **17**(12): 1685–1691

Moussion C, Ortega N, Girard JP (2008) The IL-1-like cytokine IL-33 is constitutively expressed in the nucleus of endothelial cells and epithelial cells *in vivo*: a novel 'alarmin'? *PLoS One* **3**(10): e3331

Nowinski D, Lysheden AS, Gardner H, Rubin K, Gerdin B, Ivarsson M (2004) Analysis of gene expression in fibroblasts in response to keratinocyte-derived factors *in vitro*: potential implications for the wound healing process. *J Invest Dermatol* **122**(1): 216–221

Oleinick NL, Morris RL, Belichenko I (2002) The role of apoptosis in response to photodynamic therapy: what, where, why, and how. *Photochem Photobiol Sci* **1**(1): 1–21

Osterloh A, Breloer M (2008) Heat shock proteins: linking danger and pathogen recognition. *Med Microbiol Immunol* **197**(1): 1–8

Rakemann T, Niehof M, Kubicka S, Fischer M, Manns MP, Rose-John S, Trautwein C (1999) The designer cytokine hyper-interleukin-6 is a potent activator of STAT3-dependent gene transcription *in vivo* and *in vitro*. *J Biol Chem* **274**(3): 1257–1266

Reuber MD (1961) A transplantable bile-secreting hepatocellular carcinoma in the rat. *J Natl Cancer Inst* **26**: 891–899

Riddell JR, Wang XY, Minderman H, Gollnick SO (2010) Peroxiredoxin 1 stimulates secretion of proinflammatory cytokines by binding to TLR4. *J Immunol* **184**(2): 1022–1030

Sanovic R, Krammer B, Grumboeck S, Verwanger T (2009) Time-resolved gene expression profiling of human squamous cell carcinoma cells during the apoptosis process induced by photodynamic treatment with hypericin. *Int J Oncol* **35**(4): 921–939

Seshadri M, Bellnier DA, Vaughan LA, Spernyak JA, Mazurchuk R, Foster TH, Henderson BW (2008) Light delivery over extended time periods enhances the effectiveness of photodynamic therapy. *Clin Cancer Res* **14**(9): 2796–2805

Sims GP, Rowe DC, Rietdijk ST, Herbst R, Coyle AJ (2010) HMGB1 and RAGE in inflammation and cancer. *Annu Rev Immunol* **28**: 367–388

Stathopoulos GT, Sherrill TP, Cheng DS, Scoggins RM, Han W, Polosukhin VV, Connelly L, Yull FE, Fingleton B, Blackwell TS (2007) Epithelial NF-kappaB activation promotes urethane-induced lung carcinogenesis. *Proc Natl Acad Sci USA* **104**(47): 18514–18519

Sunaga N, Imai H, Shimizu K, Shames DS, Kakegawa S, Girard L, Sato M, Kaira K, Ishizuka T, Gazdar AF, Minna JD, Mori M (2012) Oncogenic KRAS-induced interleukin-8 overexpression promotes cell growth and migration and contributes to aggressive phenotypes of non-small cell lung cancer. *Int J Cancer* **130**(8): 1733–1744

Taberner M, Scott KF, Weininger L, Mackay CR, Rolph MS (2005) Overlapping gene expression profiles in rheumatoid fibroblast-like synoviocytes induced by the proinflammatory cytokines interleukin-1 beta and tumor necrosis factor. *Inflamm Res* **54**(1): 10–16

Tracy EC, Bowman MJ, Pandey RK, Henderson BW, Baumann H (2011) Cell-type selective phototoxicity achieved with chlorophyll-a derived photosensitizers in a co-culture system of primary human tumor and normal lung cells. *Photochem Photobiol* **87**(6): 1405–1418

Wong TW, Tracy E, Oseroff AR, Baumann H (2003) Photodynamic therapy mediates immediate loss of cellular responsiveness to cytokines and growth factors. *Cancer Res* **63**(13): 3812–3818

Zheng X, Morgan J, Pandey SK, Chen Y, Tracy E, Baumann H, Missert JR, Batt C, Jackson J, Bellnier DA, Henderson BW, Pandey RK (2009) Conjugation of 2-(1'-hexyloxyethyl)-2-devinylpyropheophorbide-a (HPPH) to carbohydrates changes its subcellular distribution and enhances photodynamic activity *in vivo*. *J Med Chem* **52**(14): 4306–4318